Short-Term and Long-Term Performance of Thermosets Exposed to Water at Elevated Temperatures

S. Römhild,[1] G. Bergman,[1] M. S. Hedenqvist[2]

[1]*Swerea KIMAB, Stockholm SE-102 16, Sweden*
[2]*School of Chemical Science and Engineering, Fiber and Polymer Technology, Royal Institute of Technology, Stockholm SE-100 44, Sweden*

Received 15 May 2009; accepted 27 September 2009
DOI 10.1002/app.31548
Published online 17 December 2009 in Wiley InterScience (www.interscience.wiley.com).

ABSTRACT: The water-transport, mechanical, and chemical-structure changes in various vinyl ester, novolac, and urethane-modified vinyl ester thermosets exposed to water at 50 to 95°C for times up to 1000 days have been studied within the framework of a larger study of osmotic blistering in fiber reinforced plastics (FRP) process components. The water sorption saturation concentration did not reach a steady-state value but gradually increased in many cases upon long-term exposure. The diffusion coefficient was not significantly affected. Infrared spectroscopy and gas chromatography-mass spectrometry indicated that the net mass loss from the thermosets on immersion in water was due to the leaching of non-reacted styrene, monomer, and additives. It is suggested that this, together with polymer relaxation processes (as measured on specimens under tension in water at 80°C), is the primary reason for the time-dependent increase in the water saturation concentration. Infrared spectroscopy indicated that, even at the highest temperatures, hydrolysis of the polymer ester groups was small. Correlations were found between the styrene content in the uncured thermosets, the estimated solubility parameters, and the sorption and diffusion coefficients. © 2009 Wiley Periodicals, Inc. J Appl Polym Sci 116: 1057–1067, 2010

Key words: thermoset; transport properties; water; long-term performance

INTRODUCTION

Fiber-reinforced plastics (FRP) consisting of thermoset resins such as bisphenol A epoxy-based vinyl ester or novolac epoxy-based vinyl ester (so-called high performance thermosets) are commonly used in various types of process equipment, particularly in corrosive environments where the use of stainless steel is limited. FRP structures have become widely accepted especially in the flue gas cleaning equipment due to their good corrosion resistance and reasonable price. Although their resistance to, e.g., acids or sulfur dioxide is normally good, the diffusion of water into and through the FRP laminate may cause problems. A frequently encountered problem is deep-wall blistering. Osmotic blisters develop deep in the barrier layer of the FRP structure close to the structural laminate. In some cases, the blisters may only cause cosmetic problems, but the formation of large delamination regions and cracked blisters allowing the process environment access to the structural laminate may reduce the expected FRP lifetime. Although blistering in FRP—particularly in marine applications—has been intensively studied in recent years,[1–3] it is still a problem in FRP components in the process industry.[4–6] For this reason, the causes of blistering in high-performance FRP structures for industrial applications have been studied,[7] including the influence of material parameters such as the type of thermoset, glass fiber reinforcement/sizing, and curing systems. In addition, the influence of laminate design and environment, including water activity and temperature gradients, has been studied. Stress distributions caused by swelling and thermal expansion have been calculated. In this article, parts of this larger study and further investigations are presented. This article focuses on the short-term and long-term water transport and stability performance of various commercial thermosets between 50°C and 95°C.

Blistering in FRP structures is considered to be related to osmotic processes.[1,8–10] Water-soluble substances trapped in the thermoset initiate an osmotic process whereby water diffuses into the thermoset matrix to achieve a concentration in equilibrium with the outer environment. If the osmotic pressure becomes "too high," the laminate cracks and blisters. In high-performance FRP materials, however, other factors, including temperature and swelling gradients, also influence the blistering process.[7] The thermoset matrix may contribute to the osmotic process by the release of water-soluble substances originating from, e.g., hydrolysis of ester linkages, and it

Correspondence to: M. S. Hedenqvist (mikaelhe@kth.se).

may also influence the stress development in the laminate by its ability to absorb water. The present study of the transport and stability properties of thermosets exposed to water at elevated temperatures has been undertaken as a step towards a better understanding of the blistering phenomenon.

MATERIALS AND EXPERIMENTAL

Clear castings of commercial thermoset resins, including three types of bisphenol A epoxy-based vinyl ester resins, two types of novolac epoxy-based vinyl ester resins, a urethane-modified epoxy bisphenol A vinyl ester, and a bisphenol A fumarate-based polyester resin dissolved in styrene as co-monomer, were prepared between two glass plates covered with poly(ethylene terephthalate) (PETP) films, Table I. Figure 1 shows the general chemical structures of a bisphenol A, a novolac epoxy-based vinyl ester, and a bisphenol-A-based polyester resin. The curing system was based on a MEK peroxide dissolved in dimethyl phthalate (Norpol peroxide 11, Reichhold A/S) and a cobalt accelerator (10% cobalt octoate dissolved in high flash white spirit, Norpol accelerator 9800, unless otherwise specified). The post-curing procedure was chosen within the resin manufacturer's recommendations.

The materials were thermally characterized by differential scanning calorimetry (DSC) measurements using a Mettler Toledo 821 apparatus. A sample weighing about 8 mg was heated at 10°C/min from 25°C to 200°C in two consecutive runs. Between these heating runs, the sample was cooled to 25°C at a rate of 80°C/min.

The degree of double-bond conversion in the cured resin was determined by Raman spectroscopy using a Perkin–Elmer Spectra 2000 NIR-Raman instrument. The spectra were based on 32 scans between 4000 and 600 cm^{-1} with a resolution of 1 cm^{-1}. The degree of conversion was calculated by relating the area or height of the 1630 cm^{-1} peak (vinyl bond) to the area or height of the 1600 cm^{-1} peak (aromatic band) as proposed by Skrivars et al.[11]

The molecular weight distribution of the uncured thermoset was determined by size exclusion chromatography (SEC) using THF (1.0 mL/min) as the mobile phase at 35°C. A Viscotek TDA Model 301 instrument equipped with two GMHHR-M columns with TSK-gel (mixed bed, MW resolving range: 300–100,000) from Tosoh Biosep, a VE 5200 GPC autosampler, a VE 1121 GPC solvent pump, a VE 5710 GCP degasser, and a refractive index detector (all from Viscotel was used. A calibration method was created using narrow linear polystyrene standards. The flow rate fluctuations were corrected using toluene as internal standard. Viscotek OmniSEC version 3.0 was used to process the data. About 10 g of the

TABLE I
Curing System, Post-Curing Procedure, and Characterization of the Different Resins

Resin	Notation	Resin type	Styrene content (wt %)	Curing system	Post-curing	T_{g1} (°C)	T_{g2} (°C)	$\overline{M}_n$	$\overline{M}_w$	Degree of conversion[a] (Area/height)
Atlac 430	VE-39	Bisphenol A epoxy vinyl ester	38–41[b]	0.5% Co-solution,[c] 1.0% MEKP[d]	10 h, 100°C	115	122	975	1296	1.00/1.00
Atlac 590	NOV-37	Novolac based vinyl ester resin	35.5–38.5[b]	1.8% Co-solution, 1.0% MEKP	10 h, 100°C	128	152	897	1249	0.98/0.98
Atlac E-Nova FW 2045	VE-UR	Modified epoxy bisphenol A vinyl ester urethane resin	39–41[b]	2.0% Co-solution, 1.5% MEKP	8 h, 100°C	126	159	1455	2294	0.99/0.99
Derakane Momentum 411-350	VE-45	Bisphenol A epoxy vinyl ester	45	0.9% Co-solution, 1.0% MEKP	10 h, 100°C	115	120	1678	3139	0.99/0.99
Derakane 441-400	VE-33	Bisphenol A epoxy vinyl ester	33	1.3% MEKP, 0.12% Co-solution,[d] 0.05% DMA[e]	10 h, 100°C	121	132	1057	1511	0.99/0.99
Derakane Momentum 470-300	NOV-33	Novolac epoxy vinyl ester resin	33	0.6% Co-solution, 1.0% MEKP	10 h, 100°C	130	156	1135	1736	0.98/0.97
Atlac 382A	BIS	Propoxylated bisphenol A fumarate, unsaturated polyester resin	49–51[b]	3.0% Co-solution, 1.5% MEKP	24 h, 80°C	112	132	4026	10,204	1.00/1.00

The molecular weight in terms of $\overline{M}_n$ and $\overline{M}_w$ was obtained using styrene calibration and should be regarded as styrene equivalents.
[a] Measured by Raman spectroscopy.
[b] Solids content, IR.
[c] 1% Cobalt-octoate solution, obtained by diluting the 10% solution with styrene.
[d] 10% Cobalt-octoate solution in high flush white spirit.
[e] Dimethylaniline.

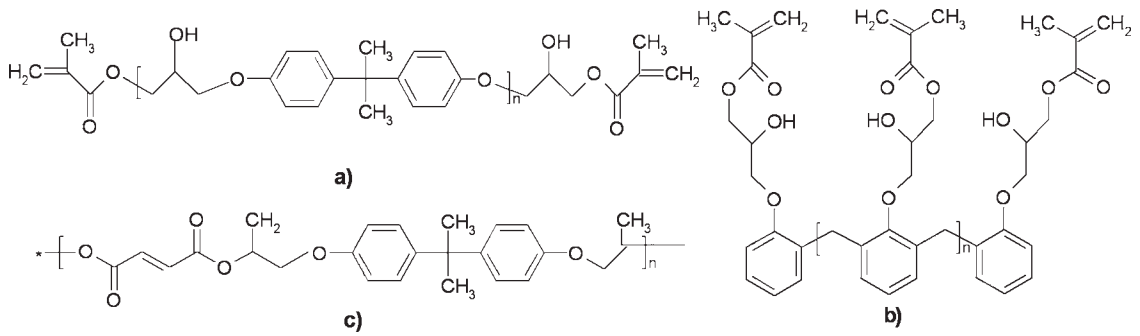

Figure 1 Chemical structures of (a) a bisphenol A epoxy-based vinyl ester resin, (b) a novolac epoxy-based vinyl ester resin, and (c) a bisphenol A fumarate-based polyester resin.

resin were dissolved in 5 mL THF (VWR, HiPerSolve Chromanorm for HPLC) and 2 mL of toluene (LabScan, HPLC grade) were added as internal standard. The baseline-corrected SEC curve was deconvoluted into Pearsson VII functions using the method of least squares, and the average molecular weight ($\overline{M}_n$) was calculated by relating the $\overline{M}_n$-value of each peak to its mass fraction defined by the area under the peak (calibration based on polystyrene standards).

To determine the short-term transport properties of water, sorption and desorption experiments were carried out at 50, 65, 80, and 95°C. Coupons 40 mm × 40 mm in size with a thickness of 4 mm were immersed in water and their mass increase was determined by intermittently weighing the surface-dried samples using a Sartorius MC 210P balance having an accuracy of 0.01 mg. Specimens of each material were exposed to water and the weight increase was measured over a time of up to 1000 days. After certain times, the sorption concentration and the mass loss were determined by desorbing the specimens. Controlled desorption experiments (single replicates) were performed by placing the specimens in an "air-conditioned" oven and then intermittently determining their weight. The water diffusivity was determined from these desorption data using Fick's second law[12]:

$$\frac{\partial C}{\partial t} = \frac{\partial}{\partial x}\left[D(C)\frac{\partial C}{\partial x}\right] \tag{1}$$

where *D(C)* is the concentration-dependent diffusion coefficient, x is the distance, and C is the concentration of water in the polymer. Only half the plate was considered; the inner boundary co-ordinate being described as an isolated point. The thickness was measured on the saturated samples, and was then assumed to be constant throughout the desorption experiment. The surface concentration was assumed to be zero during the desorption. The concentration-dependent diffusivity *D(C)*[13] was expressed as

$$D(C) = D_{C0}e^{\alpha_D C} \tag{2}$$

where D_{C0} is the zero-concentration diffusivity and α_D is the "plasticization power." Equations (1) and (2) were solved using a multi-step backwards implicit method described by Edsberg and Wedin[14] and by Hedenqvist et al.[15,16] The average diffusion coefficient $\overline{D}$ was calculated as:

$$\overline{D} = \frac{1}{C_{\max}}\int_0^{C_{\max}} D_{C0}e^{\alpha_D C}dC \tag{3}$$

where $C_{\max}$ is the maximum saturation concentration expressed as g solvent per 100 g polymer, which later is also referred to as the short-term sorption concentration C_{ST} The mass loss as a function of exposure time was calculated as

$$w_{\text{loss}}(t) = \frac{(m_0/(1 + C_{\text{initial}}/100) - m_{\text{des}}(t))}{m_0/(1 + C_{\text{initial}}/100)} \cdot 100 \tag{4}$$

where w_{loss}, m_0, C_{initial}, and $m_{\text{des}}(t)$ are, respectively, the percentage mass loss of the sample (g/100 g polymer), the initial sample weight, the initial sample water content, and the sample weight after desorption time t.

After exposure, selected resins were analyzed by infrared spectroscopy (IR) using a Bio-Rad FTS 175C FTIR spectrometer equipped with an ATR device of the Harrick's Splitpea micro-ATR type accessed with a Si ATR element. The spectra were based on 32 scans between 4000 and 500 cm^{-1} with a resolution of 4 cm^{-1}. About 8–9 g of clear castings of selected thermosets were immersed for 800 days at 95°C in about 60 mL water in glass containers. The volume of water was held constant. After the immersion, a 1 mL sample was removed and the liquid evaporated at 35°C. The residue was analyzed by IR spectroscopy using a Perkin–Elmer 1725x FTIR spectrometer equipped with an ATR system (Harrick's

Splitpea micro-ATR accessed with a Si ATR element). A spectrum based on 32 scans with a resolution of 4 cm^{-1} between 4000 and 600 cm^{-1} was obtained. Possible leaching or degradation products were extracted from 10 mL of the aforementioned aqueous solution using solid-phase microextraction (SPME) polydimethylsiloxane (7 μm) and polyacrylate (85 μm) fibers, both supplied by Supelco. The extraction temperature was 20°C and the extraction time was 30 min. The extraction products were desorbed and analyzed using a gas chromatography-mass spectrometry (GC-MS) Finnigan MAT GCQ° equipped with a non-polar column (CP-Sil 8 CB Low Bleed from Varian). The initial temperature in the column, held for 1 min, was 40°C. The temperature was then increased to 270°C at a heating rate of 10°C/min and kept at 270°C for 12 min. The injector temperature was 250°C.

Stress relaxation measurements were carried out on dumb-bell-shaped specimens (overall length 114 mm, length of the narrow section 30 mm, overall width 25 mm, width of the narrow section 6 mm) at 80°C in air and water using an Instron 5566 tensile testing machine. It was equipped with an oven in which a chamber for the water could be inserted (Fig. 2). The temperature in the water bath was regulated and controlled by an external heating device. Prior to testing, the specimens were aged in water or air at 80°C for 28 days, which was long enough to assure that at least the short-term water concentration (vide infra) had been reached. The specimens were inserted into the testing chamber, and water at a temperature of 80°C was added. The specimens were allowed to condition in the chamber for 2 h. They were then tensile strained to 0.5% (relative increase in clamp distance) using a cross-head speed of 50 mm/min and the load was thereafter measured as a function of time.

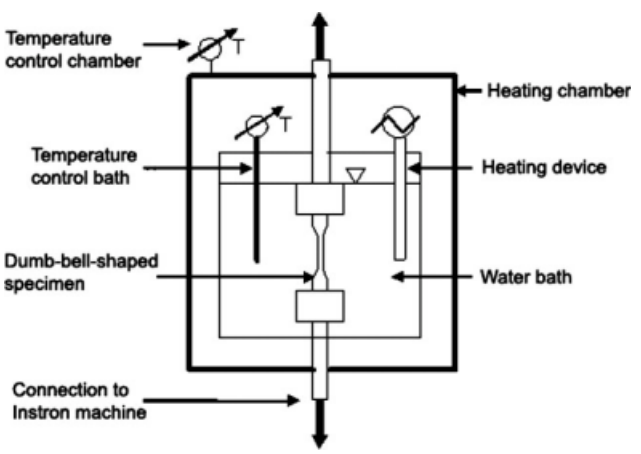

Figure 2 Experimental set-up for the relaxation test.

RESULTS AND DISCUSSION

Characterization of the material

Table I shows the T_{g1} and T_{g2} glass transition temperatures obtained from the first and second heatings in the DSC, respectively. In addition, the average molecular weights and the degree of conversion of double bonds after post-curing are given, the latter measured with Raman spectroscopy. The T_g-values indicate that none of the resins were fully cured using the recommended curing procedures. However, the residual styrene content, estimated from the T_{g1}, the DSC exotherm and the heat of styrene polymerization, was no more than ca. 0.1 wt % (weight styrene/weight cured thermoset).[17] Above a certain T_g-value, which all the clear castings exceeded, the residual styrene content decreased rapidly from over 1 wt % to 0.1 wt % or less. This is a possible explanation of why the Raman measurements indicated more or less complete conversion. To understand the relationship between the thermoset molecular structure and mobility and the transport properties, it would help to have a single parameter to represent the former properties, independent of thermoset type. It is probable that such a parameter is dependent on the number and length of the styrene crosslinks. An indirect measure of the lengths of the styrene crosslinks (probably inversely proportional to the network density) was therefore obtained by determining χ, the ratio of the number of styrene double bonds (one double bond per styrene molecule) to the number of double bonds in the pre-polymer; a ratio calculated from the styrene content and the assumed molecular structure, based on the information given by the resin manufacturers, and $\overline{M}_n$. It was here assumed that all double bonds reacted. The number of "styrene" double bonds was obtained from the styrene content in the resin mixture, and the number of double bonds in the pre-polymer was estimated from its average molecular weight and molecular structure. Since, however, the SEC-curves showed in general the coexistence of several peaks corresponding to pre-polymer chains with different numbers of repeating units, the calculation of the average molecular weight had to be simplified. The molecular weight associated with each peak was weighted by relating the area under the peak to the total area under the peaks, obtained using polystyrene standards as calibration for all the resins.

It must, however, be emphasized that the type of calibration can strongly influence the molecular weight, especially as resins with different chemical structures were studied. The Mark-Houwink constants for polycarbonate (dissolved in THF at room temperature) were used in the calculations of the molecular weights of the vinyl and bisphenol A

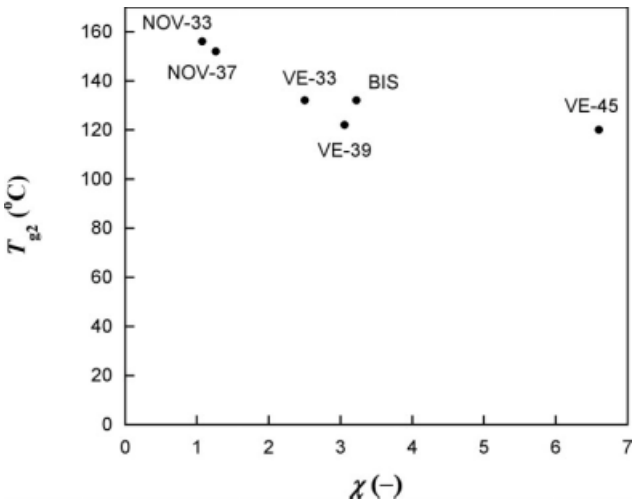

Figure 3 Glass transition temperature T_{g2} as a function of χ.

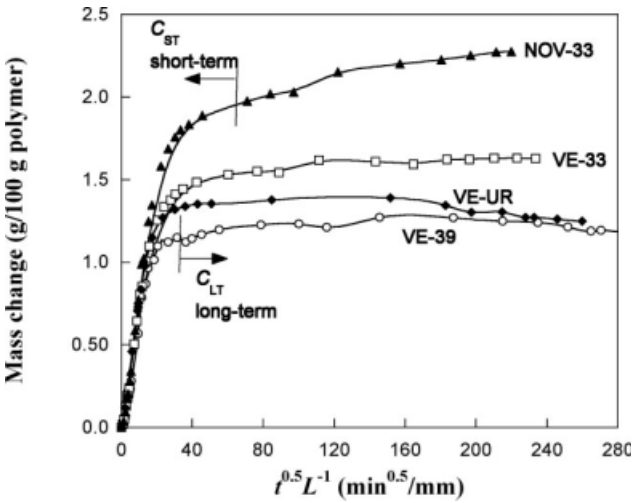

Figure 4 Typical long-term sorption curves of water for selected resins, obtained from sorption measurements at 80°C (the data have not been corrected for any leaching effects).

resins,[18] since polycarbonate was considered to have the structure most similar to these resins among those reported in the literature. The molecular weight was reduced by a factor of approximately two in comparison to the basic polystyrene calibration. This agrees well with the molecular weight reported for the Derakane 411 resin measured by SEC using epoxy for calibration.[19] To our knowledge, no Mark-Houwink constants of any polymer more similar to the chemical structure of the novolacs than polystyrene are reported in literature.

Figure 3 shows that the T_{g2}-value decreased with increasing χ ($\chi_{VE45} = 6.601$, $\chi_{VE39} = 3.060$, $\chi_{VE33} = 2.503$, $\chi_{BIS} = 3.226$, $\chi_{NOV37} = 1.266$, $\chi_{NOV33} = 1.075$), a result which could tentatively be explained as indicating that an increase in χ and thus in the length of the crosslink (number of styrene units) increases the molecular mobility and reduces molecular packing. A similar trend was observed for the vinyl ester and bisphenol A resins using molecular weights based on polycarbonate.

Short-term transport properties

The sorption curves in Figure 4 suggest that the transport properties may be time-dependent and also that several processes are occurring simultaneously in the resin. A distinction was therefore made between the short-term (ST) and long-term (LT) transport property relationship. The short-term sorption concentration C_{ST} was taken at the point where the curve was seen to reach a constant value or its slope was constant with exposure time, i.e., the increase was smaller than 0.05 wt %/h$^{0.5}$. In the case of decreasing curves, C_{ST} was determined shortly after the maximum sorption concentration had been reached. As observed in Figure 4, the sorption curves differed significantly among the resins; where the sorption curves increased, stabilized, or decreased after the C_{ST}-region. This indicates that several processes, including water sorption and the leaching of degradation products, additives and/or residual unreacted components, probably occurred simultaneously. To distinguish between these processes, the water sorption coefficient and the mass loss after drying were determined from desorption measurements at different exposure times.

In the following section, the short-term transport properties are discussed. The temperature dependence of the short-term sorption concentration, C_{ST}, is shown in Figure 5. Although a slight curvature could be observed in some cases, the relationships

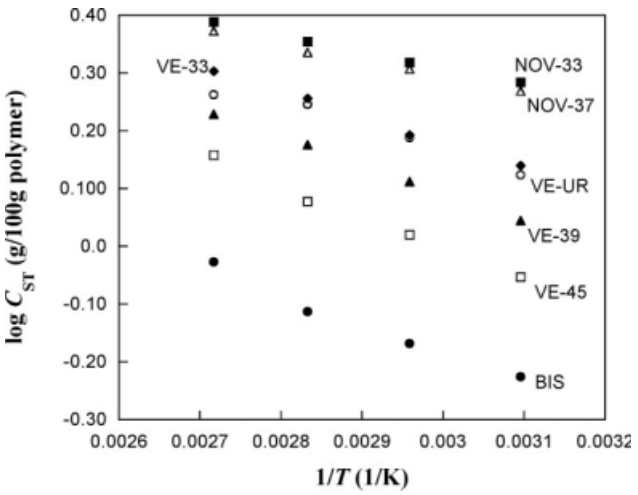

Figure 5 Arrhenius plot of the short-term sorption concentration, C_{ST}, for temperatures from 50°C to 95°C. (Reproduced from Ref. 7, with permission from Värmeforsk).

TABLE II
Parameters Describing the Arrhenius Relationships of the Short-Term Sorption Concentration C_{ST} and Average Diffusion Coefficient, $\overline{D}_{ST}$, for the Different Resins

Resin	C_0 (wt %)	ΔH_S (kJ/mol)	R^2	D_0 (cm^2/s)	ΔE_a (kJ/mol)	R^2
VE-39	36.3	9.4	0.99	1.2×10^{-2}	33.0	0.99
VE-45	42.7	10.4	0.99	1.4×10^{-2}	32.5	0.99
VE-33	31.1	8.4	0.99	1.5×10^{-3}	27.6	0.93
NOV-37	12.7	5.2	0.99	6.5×10^{-4}	25.6	0.98
NOV-33	13.7	5.3	0.99	5.1×10^{-3}	31.7	0.95
BIS	22.9	9.9	0.99	8.6×10^{-4}	22.4	0.99
VE-UR	20.1	7.2	0.98	5.6×10^{-3}	30.8	0.91

appeared to approximately follow the Arrhenius relationship:

$$C_{ST} = C_0 e^{\frac{\Delta H_S}{RT}} \quad (5)$$

where C_0 is the Arrhenius pre-exponential constant, ΔH_s is here defined as the heat of sorption, R the gas constant, and T is the absolute temperature. The pre-exponential constants and the heats of sorption for the temperature interval from 50 to 95°C are presented in Table II. The highest and lowest heats of sorption, respectively, were observed for the novolac (NOV-37) and the vinyl ester (VE-45) thermoset, both with a high styrene content. The variation in temperature-dependence was relatively small among the different thermosets. Figure 6 shows the temperature-dependence of the average short-term water diffusivity $\overline{D}_{ST}$. The diffusivity data were also fitted to the Arrhenius equation, but the fit was not as good as that for the sorption data, as indicated by the R^2-values in Table II. The Arrhenius parameters were consequently considered to be average properties within the temperature interval studied [average pre-exponential constant (D_0) and average activation energy (ΔE_D)]. Interestingly, some data seemed to describe a curved $\lg(\overline{D}_{ST}) \propto T^{-1}$-relationship, which suggests an activation energy that decreases with increasing temperature. As in the case of the sorption concentration, the variation in diffusion activation energy among the resins was relatively small. Chateauminois and Vincent[20] reported an average activation energy of the water diffusion coefficient in a bisphenol-A epoxy thermoset that decreased from 29 kJ/mol at 30°C to 27 kJ/mol at 90°C, which is within the range of values given in Table II. The concentration-dependence of the diffusivity, α_D, i.e., the "plasticization power," did not follow the Arrhenius relationship within the temperature range from 50 to 95°C, Figure 7. The ability of a solute to plasticize a polymer is believed to decrease with increasing flexibility of the polymer and, as is also shown in Figure 7, α_D did indeed decrease with increasing temperature. Another possible explanation is that α_D decreases to compensate for an increase in saturation water uptake with increasing temperature for a given thermoset. Such a compensation means that the exponent in eq. (2) is prohibited from taking very high values, and this provides a mathematical

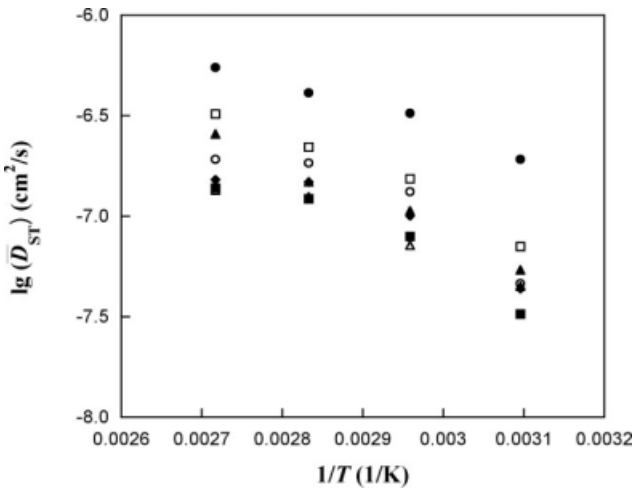

Figure 6 Arrhenius plots of the average short-term diffusion coefficient, $\overline{D}_{ST}$, between 50°C and 95°C. ■ NOV-33, △ NOV-37, ◆ VE-33, ○ VE-UR, ▲ VE-39, □ VE-45, ● BIS. (Reproduced from Ref. 7, with permission from Värmeforsk).

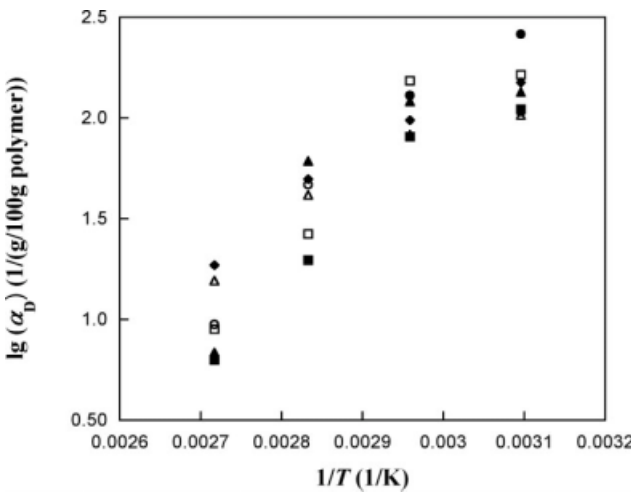

Figure 7 Arrhenius plot of α_D between 50°C and 95°C. ■ NOV-33, △ NOV-37, ◆ VE-33, ○ VE-UR, ▲ VE-39, □ VE-45, ● BIS.

rather than a physical explanation. It is difficult to determine here which of the two explanations is most appropriate or whether both apply.

In general, the short-term sorption concentration increased in the order: bisphenol A fumarate-based polyester, bisphenol A epoxy-based vinyl ester, modified epoxy bisphenol A vinyl ester urethane resin, and novolac epoxy-based vinyl ester thermosets, whereas the average diffusion coefficients followed the opposite order. To study the influence of the resin chemistry on the transport properties, the solubility parameters of the resins in terms of δ_d (contribution from dispersive forces), δ_h (hydrogen bonding forces), and δ_p (polar forces) were estimated using the method of group contributions presented by van Krevelen.[21] The molecular volume was calculated according to the group contribution method proposed by Hoy for all the resins with the exception of VE-UR, for which the molecular structure was not exactly known.[22] The number of repeating units in the pre-polymer was first estimated from the average molecular weight $\overline{M}_n$ and the solubility parameters were then calculated for an "average size" molecular structure. The solubility parameters of styrene were also calculated. The solubility parameters of the pre-polymer dissolved in styrene were then estimated based on the assumption that the parameter is proportional to the relative volume concentrations of the pre-polymer and styrene. The influence of the curing system and other additives was neglected. The estimated solubility parameters δ_d, δ_p, and δ_h for the different resins are shown in Table III. The $\Delta\delta$ for water and the thermoset systems were calculated according to:

$$\overline{\Delta\delta} = \left[\left(\delta_d^{\text{Thermoset}} - \delta_d^{\text{Water}}\right)^2 + \left(\delta_p^{\text{Thermoset}} - \delta_p^{\text{Water}}\right)^2 + \left(\delta_h^{\text{Thermoset}} - \delta_h^{\text{Water}}\right)^2\right]^{0.5} \quad (6)$$

using $\delta_d = 15.5$, $\delta_p = 16$, and $\delta_h = 42.3$ for water according to Hansen,[23] and the values obtained were then plotted against the corresponding short-term

TABLE III
Calculated Solubility Parameters Based on the Methods of van Krevelen and Hoy for the Different Resin Systems Studied

	δ_d	δ_p	δ_h
VE-39	20.37	2.44	11.33
VE-45	20.60	2.09	11.21
VE-33	20.42	2.38	11.43
NOV-37	20.20	3.27	12.51
NOV-33	20.35	2.89	12.89
BIS	21.73	1.62	8.44
Water[20]	15.5	16	42.3

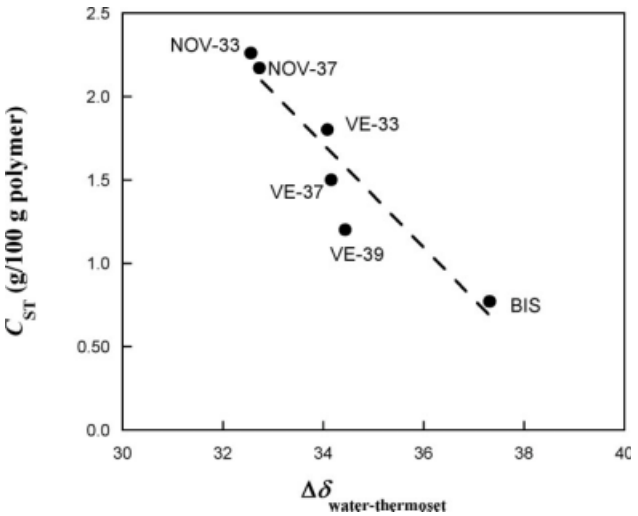

Figure 8 Short-term sorption coefficient of water, C_{ST}, at 80°C versus the water-polymer solubility parameter difference.

sorption concentration at 80°C, Figure 8. An approximately linear relationship was obtained. Similar linear relationships were observed at the other temperatures (data not shown). As discussed previously, the molecular weight used as a basis for the solubility calculations is dependent on the type of calibration. A sensitivity analysis was carried out where the molecular weight of the resins was reduced by different factors and where a calibration based on polycarbonate was used for the vinyl and the bisphenol A resins leaving the molecular weight for the novolacs unchanged. In all cases, trends similar to those shown in Figure 8 were observed. An explanation may be found in Figure 9(a,b), which show the short-term sorption concentration (C_{ST}) and the short-term zero-concentration and average diffusion coefficients ($D_{C0,ST}$ and $\overline{D}_{ST}$) of water plotted against the styrene concentration in the uncured resins (at 80°C). The short-term sorption coefficient decreased as a linear function of increasing styrene content within the studied region, which may possibly be explained by the decrease in thermoset polarity as reflected by the values of δ_p and δ_h (Table III). At the same time, the diffusion coefficient increased with increasing styrene content, and thus with decreasing content of oxygen or oxygen-containing polar groups in the polymer; an effect which has been suggested to be due to a dilution of "barrier-acting" water-polymer hydrogen-bonds.[24] A decrease in crosslink density may also lead to an increase in molecular mobility and free volume, reflected in an increasing water solubility and diffusivity. However, assuming that the crosslink density was correlated directly with χ, it was found that, although the diffusivities ($D_{0,ST}$ and $\overline{D}_{ST}$) increased with χ, C_{ST} followed an opposite trend (data not

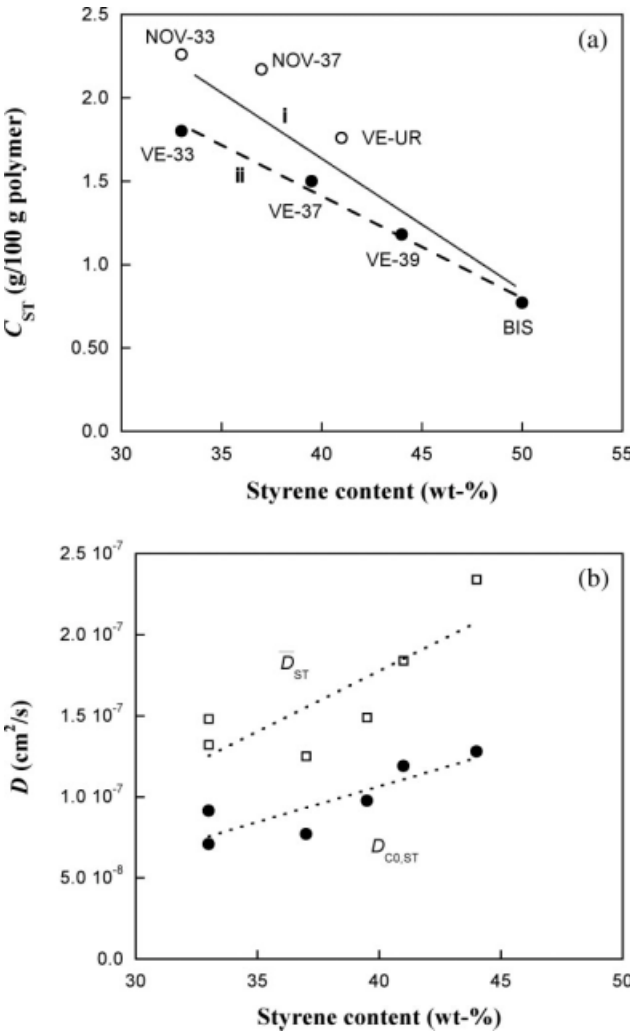

Figure 9 Dependence on the styrene concentration in the resin of (a) the short-term sorption concentration, C_{ST}, and (b) the short-term zero-concentration, $D_{C0,ST}$, and average diffusion coefficient, $\overline{D}_{ST}$, of water at 80°C in different resins. In Figure 9(a), line (i) represents the average relationship for all resins whereas line (ii) shows the relationship between the sorption coefficient and the styrene content only for the bisphenol A based resins (●). ○ denotes all other resins.

shown). Consequently, the polarity of the thermoset (depending on the styrene content) seemed to be the major factor affecting the solubility whereas also crosslink densities may have been important for the diffusivity.

To study in more detail the effect of the degree of curing on the transport properties, clear castings of the novolac resin NOV-33 were subjected to different post-curing procedures including post-curing at 100°C for 10 h, at 100°C for 10 h followed by 2 h at 120°C and at 100°C for 10 h followed by 3 h at 150°C. The T_{g1} for these resins was found to be 130, 140, and 158°C, respectively. The sorption coefficient decreased slightly with increasing T_{g1}-value from 2.26 wt % for a T_{g1} of 130°C to 2.01 wt % for a T_{g1} of 158°C, whereas the diffusion coefficient was not significantly affected. Hence, within the limits tested here, the degree of curing seemed to have only a slight effect on the water transport properties. This is in agreement with the data suggesting that it is mainly the styrene content (change in thermoset polarity) that affects the water transport properties. It should be pointed out that a different result might be obtained for a non- or slightly post-cured resin.

Long-term transport performance

Materials were subjected to long-term water exposure at temperatures between 50°C and 95°C to study the thermoset stability and the time-dependence of the transport properties. The long-term sorption concentration increased with increasing exposure time for all resins at 95°C, as shown in Figure 10. At lower temperatures (50–80°C), the increase in sorption concentration with time seemed to be smaller, although this was difficult to evaluate quantitatively. The water diffusivity at 80°C was determined from desorption measurements, starting at different exposure times, for the resins VE-45 and VE-39. The slight decrease in diffusion coefficient observed with increasing exposure time was not statistically significant.

Mass loss curves after long-term immersion in water at 95°C are shown in Figure 11. At 95°C, almost all the resins showed an approximately linear decrease in mass with time. Among the thermosets tested, the bisphenol A polyester (BIS) and the urethane modified vinyl ester (VE-UR) showed the highest mass loss. The mass loss of the resins at 80°C was less than 0.2 wt % after 950 days of

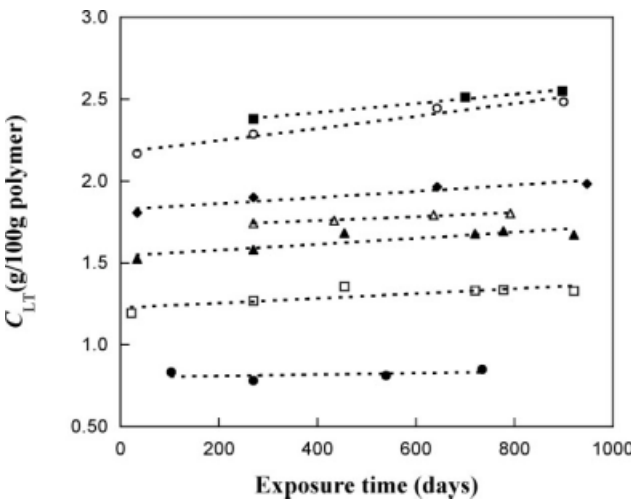

Figure 10 Long-term sorption concentration in water, C_{LT}, at 95°C versus exposure time. ■ NOV-33, ○ NOV-37, ◆ VE-33, △ VE-UR, ▲ VE-39, □ VE-45, ● BIS. (Reproduced from Ref. 7, with permission from Värmeforsk).

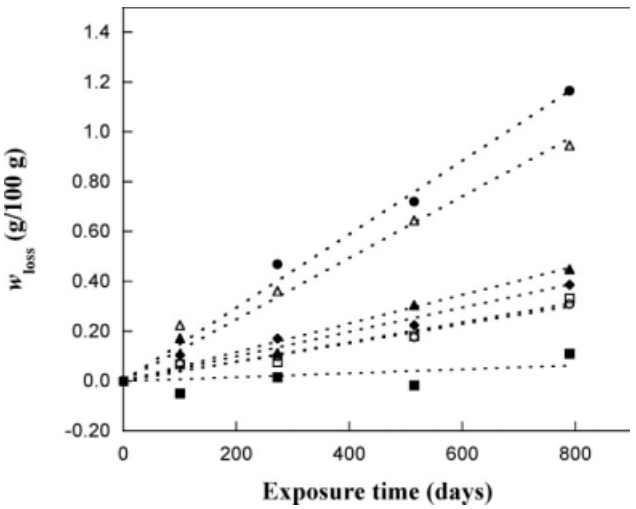

Figure 11 Mass loss versus exposure time in water at 95°C. ■ NOV-33, ○ NOV-37, ◆ VE-33, △ VE-UR, ▲ VE-39, □ VE-45, ● BIS. (Reproduced from Ref. 7, with permission from Värmeforsk).

exposure (data not shown). In general, the novolac-based vinyl ester resins (NOV-33 and NOV-37) exhibited a smaller mass loss than the other resins. At 65°C and 50°C, the mass loss was negligible (data not shown). To reveal whether hydrolysis played an important role in the mass loss, the relative concentration of ester groups was estimated with IR, Figure 12. Characteristic ester absorption bands are located at 1730 and 1296 cm^{-1}. The peaks at 700 and 1510 cm^{-1} were chosen as reference peaks (carbon–carbon vibrations in aromatic rings).[25,26] The 1296 cm^{-1} peak normalized with respect to the 700 cm^{-1} peak was found to be the most suitable indicator of the presence of ester groups. At 95°C, a small decrease in the ester concentration was observed, indicating a certain degree of hydrolysis. At 80°C, the decrease was even smaller or absent. Overall, the small decrease in ester concentration suggests that hydrolysis was not a primary cause of the mass loss. To determine what compounds were leaving the samples during the long-term exposure at 95°C, aqueous solutions in which selected resins had been immersed for 800 days were analyzed with IR and GC-MS. The IR results indicated that the aqueous solutions associated with the VE-45 and NOV-33 resins, having a pH of about 3, contained carboxylic acid (1703 cm^{-1}) and Si—O groups (1045 cm^{-1}). In addition, peaks appearing at 700 cm^{-1} and 1510 cm^{-1} indicated the presence of aromatic compounds. The GC-MS screening indicated the presence of benzoic acid and other styrene derivatives, bisphenol A, phthalates, a long-chain fatty acid derivative, and siloxane-containing compounds. These compounds were not positively identified. Benzoic acid and its derivatives can form during the oxidation of styrene. To our knowledge, the resins did not contain any Si—O-containing additives, but the Si—O species could have originated from the glass container in contact with the acidic solution containing the samples. To conclude, it seemed that the main reason for the mass loss observed at 95°C was the loss of styrene, resin pre-polymers, and phthalate-based additives, the latter originating from the curing system.

Stress relaxation measurements

It is possible that the increase in sorption coefficient with time was due to stress relaxation processes taking place in the polymer. The relaxation behavior was therefore investigated for selected specimens aged in water and air, respectively, at 80°C for 28 days. The novolac (NOV-33), the vinyl ester (VE-33), and the urethane-modified vinyl ester (VE-UR) resins were chosen, since these showed differences in long-term water sorption behavior at elevated temperature, Figure 4. The novolac resin exhibited a significant increase in sorption concentration, the vinyl ester a much smaller increase, and the urethane-modified vinyl ester a decrease in sorption concentration with time, as measured using sorption and neglecting leaching effects. Figure 13(a) shows the relaxation curves of the VE-UR resin in air and water. After a rapid initial stress decay in both air and water, the further stress relaxation over longer times was more pronounced in water. The presence of water seemed to increase the relaxation strength, possibly due to its plasticization effect. The stress relaxation behavior was quantified using a Maxwell two-element model[27]:

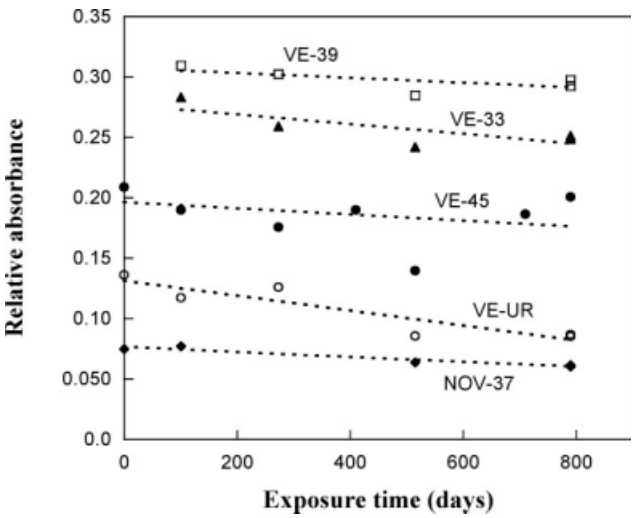

Figure 12 Intensity of the 1296 cm^{-1} band normalized with respect to the intensity of the 700 cm^{-1} band for selected resins at 95°C. (Reproduced from Ref. 7, with permission from Värmeforsk).

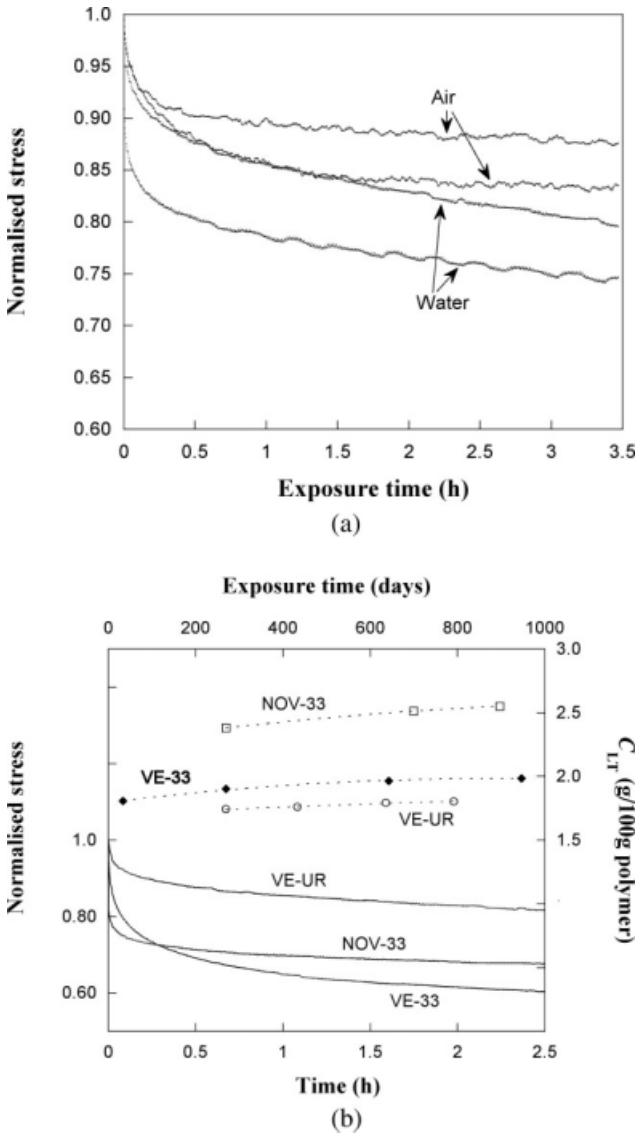

Figure 13 (a) Normalized stress relaxation curves for VE-UR specimens exposed to air and water at 80°C. (b) Comparison between the time-dependence of the long-term sorption coefficient and the normalized relaxation curves obtained in water at 80°C.

$$\sigma(t) = \sum_i \sigma_i e^{\frac{t}{\tau_i}} \quad i = 2 \tag{7}$$

where σ_i are the stress components, τ_i the relaxation times, and t the time. The data were fitted using the least squares method and the results are summarized in Table IV. The relaxation time τ_2, describing the long-term relaxation behavior, was somewhat higher for specimens exposed to water than for those exposed to air in the case of the VE-UR and VE-33 resins, but similar for the NOV-33 resin. Figure 13(b) shows a comparison between the relaxation behavior of the resins aged in and exposed to water during the stress relaxation test and the long-term sorption behavior. It was expected that the novolac resin NOV-33 would show the most pronounced relaxation effect in water since the sorption coefficient displayed the greatest time-dependence. There seemed, however, to be no clear correlation between the stress relaxation and long-term sorption behavior of the samples. Topíc and Katović[28] reported that the presence of water in a novolac phenol formaldehyde resin induced changes in the β relaxation and relieved motions of certain molecular groups in the resin. It is worth noting that De Wilde and Shopov[29] have proposed a model to describe moisture sorption in epoxy resin, based on Fickian diffusion and stress relaxation effects, which shows a long-term sorption behavior similar to that observed here.

Fedor[30] suggested that the increase in the sorption concentration above C_{LT} is caused by osmotic processes, which implies that the sorption in a polymer can be divided into two parts, the short-term behavior (up to C_{LT}) being determined by the solubility parameters of the solute and polymer, and the increase in the sorption concentration beyond C_{LT} being related to the presence of water-soluble degradation products trapped in the polymer which initiate osmotic processes and are the driving force for additional water to diffuse into the polymer. The results obtained in this study indicate, however, that the mass loss at elevated temperature is primarily related to the loss of unreacted styrene, pre-polymers, and additives and that the effect of hydrolysis is small. In addition, the presence of water initiated stress relaxation processes in the resin. Hence, in this case, it is more probable that relaxation processes and the loss of "unbonded" species, allowing more water to enter, were the primary reasons for the increase in the sorption concentration. Fedor's sorption model is more applicable to water sorption in more hydrolytically unstable resins such as the ortho-polyester resin. In that case, the sorption curve showed a significant increase at the point at which hydrolysis started and disc cracks were

TABLE IV
Relaxation Data Quantified Using a Two-Element Maxwell Model

Material	Environment	σ_1 (MPa)	τ_1 (h)	σ_2 (MPa)	τ_2 (h)
VE-UR	Water	2.48	36.56	0.26	0.12
		2.06	30.60	0.18	0.16
	Air	2.08	87.53	0.16	0.12
		2.06	87.53	0.25	0.34
VE-33	Water	1.44	16.49	0.36	0.11
		2.61	16.97	0.45	0.16
		1.66	18.66	0.47	0.21
	Air	0.90	23.75	0.29	0.98
		2.16	93.98	0.14	0.19
NOV-33	Water	2.35	42.02	0.22	0.18
		2.04	60.44	0.23	0.17
	Air	2.07	62.11	0.20	0.19
		2.84	40.35	0.27	0.15

formed (data not shown). In this work, physical processes which may occur during aging of the resin, other than those related to stress relaxation, have not been considered or studied. Physical ageing below the glass transition temperature may lead to an embrittlement of the resin matrix. A common explanation for the embrittlement is chemical degradation reactions and the leaching of low molecular weight compounds, which otherwise help to plasticize the resin matrix.

CONCLUSIONS

The transport properties of water in different thermosets have been adequately related to their chemical structure using the solubility parameter concept, based on information relating to the chemical structure, the styrene content, and the average molecular weight (styrene equivalents). The short-term water sorption concentration increased approximately as a linear function of increasing solubility parameter, i.e., increasing polarity or decreasing styrene content, whereas the diffusivity decreased. Further, the long-term water sorption concentration was found to be time-dependent, increasing with increasing exposure time in the 50–95°C temperature range up to times of 1000 days. The long-term diffusivity was not, however, significantly affected within the actual exposure time-interval. The increase in the long-term sorption coefficient with time seemed primarily to be related to stress relaxation processes in the polymer as indicated by relaxation measurements in water at 80°C, for which the stress relaxation was greater than in the dry material at this temperature, and certain leaching effects. Although a certain mass loss was observed on long-term exposure above 80°C, IR measurements and GC-MS screening indicated that most of the mass loss during water exposure was due to the leaching of non-reacted styrene, pre-polymer, and additives. Further, IR measurements indicated that hydrolysis of the ester groups was only small at elevated temperatures.

The authors thank the Swedish Association for Thermal Research (Värmeforsk), the Swedish Knowledge Foundation (KK-stiftelsen), Ashland Composite Polymers, DSM Resins B.V., Owens-Corning Sweden AB, Saint Gobain Vetrotex International, Sunila Oy, Termap AB, and Plastilon Oy for their financial support. They also thank Annika Lindström at KIMAB, Stockholm, and Daniel Nyström at KTH, Stockholm, for help with the GC-MS measurements and the SEC-measurements, respectively.

References

1. Ghotra, J. S.; Pritchard, G. Osmotic Blister Formation in FRP Laminates, 28th National SAMPE Symposium, Anaheim, California, April 12–14, 1983.
2. Burrell, P. P.; Herzog, D. J.; McCabe, R. T. A Study on the Permeation Barriers to Prevent Blisters in Marine Composites and a Novel Technique for Evaluation of Blister Formation, 42nd Annual, 1987, SPI Conference Section Marine, Session 15-e.
3. Bogner, B. R.; Edwards, H. R. The Cost/Performance Advantages of Isophthalic Based Acid Unsaturated Polyesters in Gel Coated Laminates, Composites Institute's 51st Annual Conference and Exposition 1996, February 5–7, 1996, Cincinnati, Ohio, Session 12.
4. Bergman, G.; Petterson, K. Investigation of Blistering and Delamination Damage in a Flue Gas Scrubber Made of Glass-Fiber Reinforced Ester Plastics (FRP), Project report 66 231:E; Swedish Corrosion Institute: Stockholm, Sweden, 1994.
5. Bergman, G. Blistering Damage in a Flue Gas Scrubber Made of Glass-Fiber Reinforced Ester Plastics (FRP), Project report 66 229–1E; Swedish Corrosion Institute: Stockholm, Sweden, 1995.
6. Römhild, S.; Bergman, G. Investigation of Extensive Deep-Wall Blistering Damage to FRP Process Piping in the Bleach Plant at Sunila Mill, Report C 2003:1; Swedish Corrosion Institute: Finland, 2003.
7. Römhild, S.; Bergman, G.; Eriksson, P. Blistering in Constructions of Fiberglass Reinforced Plastics (FRP)—Causes and Countermeasures, Värmeforsk project report M4–307/M5–501, Sweden, 2005.
8. Davis, R.; Ghotra, J. S.; Pritchard, G. Blister Formation in RP: The Origin of the Osmotic Process, 38th Annual Conference; Reinforced Plastics/Composites Institute, Houston, Texas, February 7–11, 1983.
9. Gothra, J. S.; Pritchard, G. Developments in Reinforced Plastics - 3, Elsevier Applied Science Publishers: London and New York, 1984, p 63–95.
10. Chen, F.; Birley, A. W. Osmosis and Blistering in FRP, Handbook of Polymer-Fiber Composites; Longman Scientific & Technical; Harlow: Essex, England, 1994.
11. Skrivars, M.; Niemelä, P.; Koskinen, R.; Hormi, O. J Appl Polym Sci 2004, 93, 1285.
12. Crank, J. The Mathematics of Diffusion; Clarendon Press: Oxford, 1986.
13. Hedenqvist, M. S.; Yousefi, H.; Malmström, E.; Johansson, M.; Hult, A.; Gedde, U. W.; Trollsås, M.; Hedrick, J. L. Polymer 2000, 41, 1827.
14. Edsberg, L.; Wedin, P. Å. Optim Meth Softw 1995, 6, 193.
15. Hedenqvist, M. S.; Ohrlander, M.; Palmgren, R.; Andersson, A. C. Polym Eng Sci 1998, 38, 1313.
16. Hedenqvist, M. S.; Tränkner, T.; Varkalis, A.; Johansson, G.; Gedde, U. W. Thermochimica Acta 1993, 214, 111.
17. Bergman, G. Studies on the Glass Transition Temperature, T_g, and the Degree of Cure of Postcured and Non-Postcured Vinylester and Bisphenol A-Polyester Resins, Project report 66 197:1; Swedish Corrosion Institute: Stockholm, Sweden, 1992.
18. Brandrup, J.; Immergut, E. H.; Grulke, E. A., Eds. Polymer Handbook, 4th ed.; Wiley & Sons: New York, 2005; Chapter 7.
19. La Scala, J. J.; Orlicki, J. A.; Winston, C.; Robinette, E. J.; Sands, J. M.; Palmese, G. R. Polymer 2005, 46, 2908.
20. Chateauminios, A.; Vincent, L. Polymer 1994, 35, 2.
21. Van Krevelen, D. W. Properties of Polymers, 3rd ed.; Elsevier: Amsterdam, 1990.
22. Hoy, K. L. J Paint Technol 1970, 42, 76.
23. Hansen, C. Hansen Solubility Parameters: A User's Handbook; CRC Press: Boca Raton, Fla, 2000.
24. Bellenger, V.; Verdu, J.; Ganem, M.; Mortaigne, B. Polym Polym Comp 1994, 2, 1.
25. Bélan, F.; Bellenger, V.; Mortaigne, B. Polym Degrad Stab 1997, 56, 93.
26. Becart, D.; Mariette, B.; Hoarau, P.-A.; Guerin, P. Eur Polym J 1998, 34, 5/6, 747.
27. Ward, I. M. Mechanical Properties of Solid Polymers; Wiley: New York, 1985.
28. Topić, M.; Katović, Z. Polymer 1994, 35, 25, 5536.
29. De Wilde, W. P.; Shopov, P. J. Compos Struct 1994, 27, 243.
30. Fedor, R. F. Polymer 1980, 21, 207.